© 2018 IJSRST | Volume 4 | Issue 5 | Print ISSN: 2395-6011 | Online ISSN: 2395-602X
Themed Section: Science and Technology

Petrographical and Mineralogical Characteristics of Bauxite Deposit of Darai-Daldali Plateau, Kabirdham district, Chhattisgarh

Bhumika Das, M. W. Y. Khan
School of Studies in Geology and Water Resource Management, Pt. Ravishankar Shukla University, Raipur, Chhattisgarh, India

ABSTRACT

This paper embodies the results of petrographical and mineralogical investigations carried on bauxite deposit of Darai-Daldali plateau, Kabirdham district, Chhattisgarh. Representative samples of bauxite, lateritic bauxite and laterite were studied to know petrographic and mineralogical variation. Microscopic examinations show pelitomorphous-collomorphous texture, due to colloidal precipitation. The XRD data reveal abundance of gibbsite in bauxite samples, followed by anatase, brookite and kaolinite, while lateritic bauxite and laterite samples are enriched in goethite, hematite and anatase in addition to gibbsite. Results of DTA/ TG and FTIR analysis confirmed the absence of boehmite. Minor variation in DTA/TG peaks most probably accounts for the variation in sample quantity taken for analysis.

Keywords : Bauxite, Laterite, Gibbsite, Daldali, Weathering, Kabirdham.

I. INTRODUCTION

Bauxite is not a mineral, it is a rock formed from laterite or lateritic soil that has been severely leached of silica and other soluble materials of variable composition, in a wet tropical or subtropical climate. Rao and Krishnamurthy (1981) mention a diverse parentage of Indian bauxite deposits, such as Khondalites and Charnockite (East coast Bauxites); granite and gneisses (Western Ghat Bauxites); Upper Vindhyan sandstones (deposits of U. P.) and Deccan Trap basalts (Bauxites of central India). Although bauxites of basaltic parentage have been studied widely, however variation in mineralogical and petrographic characters of one deposit to other is obvious due to variable conditions of diagenetic/epigenetic processing. Keeping above in view, the present paper presents petrographic and mineralogical characters of the Dari-Daldali bauxite deposit of Kabirdham district, Chhattisgarh, and attempts to discuss their genetic control.

II. GEOLOGICAL SETUP

The present study area lies in SOI toposheet no 64 F/3 and is bounded by latitudes 22° 22'30" to 22° 27'30"N and longitudes 81° 10'00" to 81° 12'30"E, having maximum elevation of 940 m above mean sea level. Deccan lava flows capped by laterite and lateritic bauxites constitute the topmost geological formation, unconformably overlying the slates and phyllites of Chilpi Group. The Deccan lava flows which are almost horizontally disposed are fine grained and generally massive. Columnar jointing is well developed at places. The total thickness of laterite is about 15 - 30 m in Darai-Daldali plateau and comprises several recognizable lithological units (Figure 1). The low lying areas and interfluves of small streams are occupied by phyllites, slates with interbedded quartzite of Chilpi Group (Middle Proterozoic). The

rocks of Chilpi Group unconformably overly the Nandgaon Group.

III. METHODOLOGY

For present study we collected samples from quarry faces as well as drill-hole cores,

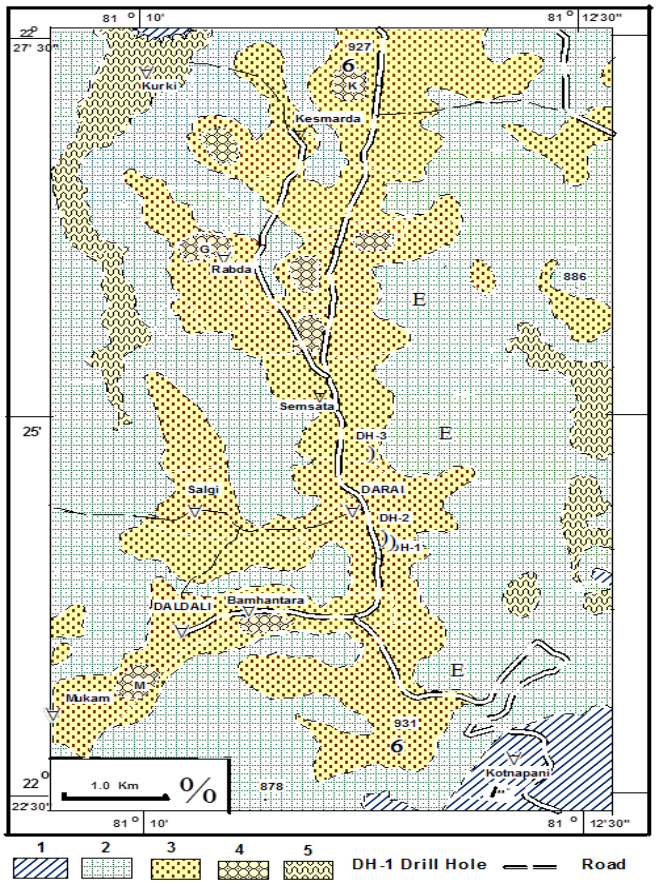

Figure 1. Geological map of Darai-Daldali plateau.

representing vertical profile; belonging to bauxite, lateritic bauxite and laterite. XRD, Infra-red spectroscopy and TGA DTA analyses were carried out at Institute of Minerals and Materials Technology (CSIR) Bhubaneswar.

Mineral phase identification is carried out using a Philips X-ray Diffractometer (PW-1710) having graphite monochromatic assembly. CuKα radiation operating at 40 kV and 20 mA current was used for this purpose. A diffraction pattern recording the angle 2θ against the intensity was obtained over a range between 10^{o} and 70^{o}. The scanning rate was 2^{o} per minute with recorder full scale set into 2 x 10^{3} counts. Some samples were also analysed at NIT, Raipur and at PRSU, Raipur. To study structural behavior of various chemical groups in our samples, FTIR spectra were obtained on selected samples using Perkin Elmer spectrum- GX, under electro-magnetic spectrum: ~4000 cm^{-1} to 200 cm^{-1}. To observe changes in physical and chemical properties of materials as a function of increasing temperature, differential thermal analysis (DTA) and thermo gravimetric analysis (TGA) were undertaken using Mettle-Toledo thermal analyzer at IMMT, Bhubaneswar.

IV. RESULTS

A. PETROGRAPHY

The bauxite of Darai, Daldali plateau belongs to lateritic type, developed as a result of leaching of silica and other soluble constituents from basalts of Deccan Trap. A well developed lateritic profile (Figure 2) comprises lateritic soil / compact laterites lateritic bauxite and bauxite downward. In drill-hole samples lithomarge is also encountered below laterite. Based on field studies bauxites and lateritic bauxites are differentiated on the basis of colour.

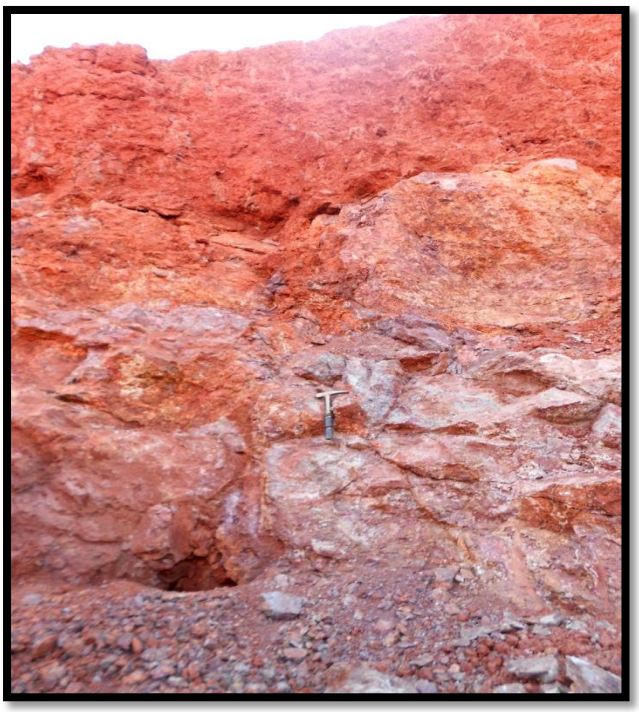

Figure 2. Field photograph showing laterite profile having well developed boulder bauxite horizon, underlain by lateritic soil.

In hand specimen bauxite appears reddish white massive to mottled (collomorphous) (Figure 3) and granular in nature while lateritic bauxite is texturally massive to pisolitic (Figure 4). Under microscope, collomorphous-pelitomorphous and pisolitic textures are very well observed in this bauxite.

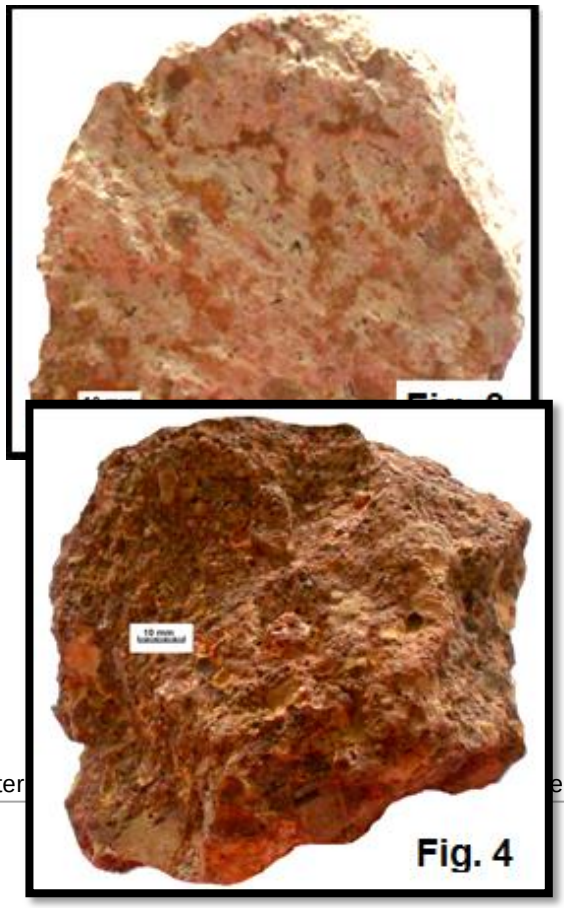

Figure 3. Bauxite ore showing mottled texture in hand specimen.

Figure 4. Hand specimen of lateritic bauxite showing pisolitic texture.

Microscopic examination of the bauxite samples was done both under transmitted and reflected light to study micro texture and fabric. Collomorphous-pelitomorphous texture (similar to 'Gel-like texture' by Valeton 1972) is mainly found in massive and mottled ores (Fig 5), whereas pelletal and pisolitic texture in mottled bauxite ores. The collomorphous texture is also reported from laterite type bauxites by Rao and Krishnamurthy 1981, Jing at el 2013, and many others. Development of micro cavities in massive bauxites probably due to desiccation of colloidal deposits is observed in some samples. The cavity walls are also show colloidal bands and gibbsite aggregate (Figure 6).

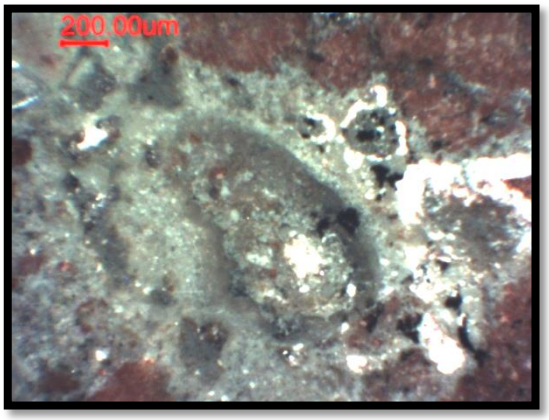

Figure 5. Optical micrograph showing collomorphous texture, wherein segregation of goethite (brownish) and gibbsite (grayish) is observed. Bright white is hematite. Note colloform banding in the centre. Under reflected light cross polars.

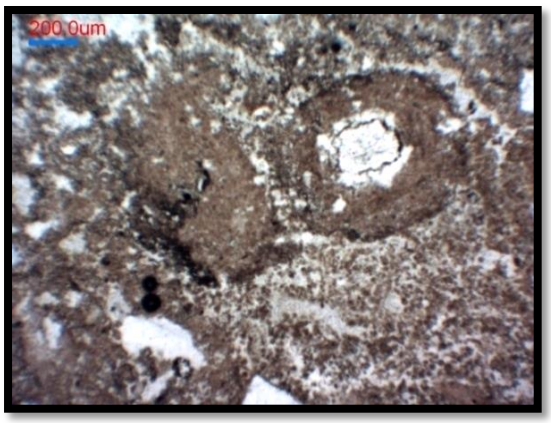

Figure 6. Optical micrograph showing pelletal texture in bauxite. Note occurrence of pisolite showing development of gibbsite (white coloured) in the centre. Transmitted plane polarized light. Bar scale 200 μm.

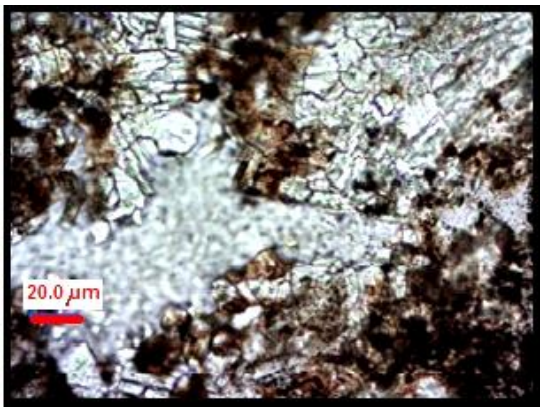

Figure 7. Optical micrograph showing well developed subhedral hypidiomorphic gibbsite crystallites masked with goethite (brownish coloured) and a cavity filled with amorphous clay. Under transmitted polarized light.

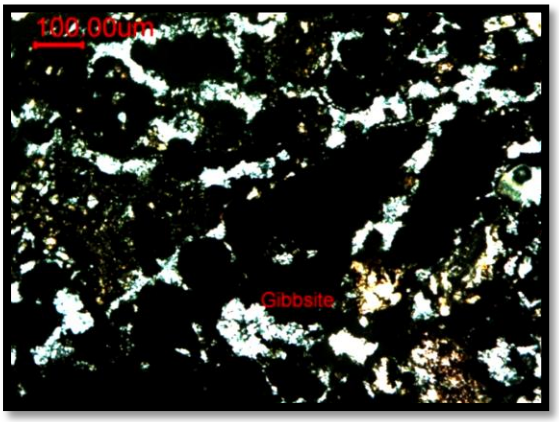

Figure 8. Optical micrograph showing goethitic pisolite and lumps (centre), along with gibbsite occurring in interstitial spaces. Transmitted cross polars.

Remobilization of aluminous solutions and precipitation of subhedral hypidiomorphic gibbsite indicative of epigenesis is a commonly observed textural feature in massive bauxite (Fig. 7). Pisolitic texture is very well observed in lateritic bauxites, due to occurrence of goethitic pisolites varying in size from 100 to 150 microns along with gibbsite infilling the interstitial spaces (Fig. 8). At places development of gibbsite pisolites due to replacement of goethite is also observed.

.

B. MINERALOGY

XRD analysis of bauxite, lateritic bauxite and laterite samples demonstrates presence of only gibbsite in bauxite samples, while abundance of gibbsite decreases towards laterites with the increase of hematite, goethite, kaolinite, anatase, brookite and quartz (Table – 1 A and B).

The results of simultaneous thermal analysis (DTA and thermo gravimetric analysis) are presented in Table - II. Deer et al. (1975) have reported strong endothermic peak at 300 - 342 ^{o}C for gibbsite. I n case of present study, the DTA curves of the bauxite samples (B1 B2 & B5) show sharp endothermic peaks varying from 300^{0}C to 325^{0}C, related to the transformation of gibbsite into the first meta stable alumina phase (x-Al2O3) and predominance of gibbsite mineral phase. The Thermogravimetry curves of above samples show a corresponding rise in temperatures of transformation and cumulative weight loss up to a maximum temperature varying between 510^{0}C to 540^{0}C. The net weight loss due to release of hydroxyl ion in gibbsite samples varies from 25.96% (B1) to 28.19% (B5). In lateritic bauxite (LB-3) and laterite samples (L-4) sharp endothermic peaks are recorded at 315 ^{0}C and 310 ^{0}C respectively, suggesting

dominance of gibbsite. The endothermic peaks in all samples indicate presence of gibbsite phase only. However, minor variation in the values of endothermic peaks, most probably accounts for variable initial weight of the samples taken for DTA and TGA analysis. This contention is also supported by the results in Table- II. As sample B-1 has highest initial weight but lowest weight loss when compared to sample B-5 having lowest initial weight but highest weight loss.

IR spectroscopy helps in distinguishing mineral phases accurately on the basis of their internal structure and nature of bonding (Raun et al 2001). In infrared spectra (Table –III) bands are observed in three vibrational modes at *v* (OH), δ OH and γOH for gibbsite. The standard OH and Al-O-H stretching and bending frequencies are compared with observed frequencies in our samples (Table - III). In the samples of present study, v(OH) bands are observed at 3622 to 3626 cm^{1} frequencies corresponding to 3617 bands of gibbsite (Raun at all 2001). The hydroxyl deformation peaks corresponding to 1060, 1024 and 914 cm^{-1} are found to vary from 1013 to 1061 cm^{-1}, confirming the presence of gibbsite. In some samples (LB-12, LB-15, G5, LB-3, L-4, LB-6, L-7) *v* (OH) stretching bands is observed at 3700 to 3694 cm^{-1} along with H-O-H banding at 1632 to 1642 cm^{-1}, and Si-O vibration bands at 1111 to 1117 cm^{-1} frequency accounting for the presence of kaolinite. Presence of quartz is also inferred on the basis of 709 to 720 cm^{-1} frequency bands typical of Si-O vibration for quartz, further presence of goethite is also confirmed by the occurrence of 896 to 981 cm^{-1} frequency peaks. The above IR spectral data do not show any peaks for Boehmite and Diaspore in these samples, which is in confirmation with XRD results (Table-I A and B).

DISCUSSION

The textural studies of bauxite ores, lateritic bauxite and laterite from present study area clearly demonstrate the role of weathering processes in the development of lateritic profile. The collomorphous-pelitomorphous texture in bauxite samples is due to colloidal precipitation of Al^{+3} hydroxyl gel. The pisolitic texture showing replacement of goethite by gibbsite is a result of leaching of iron during late stage of bauxitization. The XRD data reveal that this deposit is characterized by the abundance of aluminum trihydrate (gibbsite) mineral phase only, which is also supported by DTA/TG and IR studies. Since Diaspore is considered as a product of diagenetic weathering (Kloprogge et al, 2002), therefore its absence in Daldali Bauxite, suggests that this bauxite is a product of pedogenic weathering process, which is also supported by petrographic studies.

Table 1. A: XRD Data of representative samples

Mineral Phase	DN4W8-1(B-1)		DN4W8-2(B-2)		DN4W8-3(LB-3)		Min. Phase	DN5W6 (i) B-5		DN5W6 (iii) L-7	
	dÅ	Rel. Int.	dÅ	Rel. Int.	dÅ	Rel. Int.		dÅ	Rel. Int.	dÅ	Rel. Int.
Ka	-	-	-	-	-	-	**Ka**	-	-	7.191	52.02
Gi	4.837	100.00	4.837	100.000	4.834	100.000	**Gi**	4.851	100.000	4.848	58.660
Gi	4.376	22.080	4.380	-	4.376	-	**Gi**	4.388	21.280	-	-
Gi	-	-	4.363	33.560	4.362	3.320	**Go**	-	-	4.157	92.510
Go	-	-	-	-	-	-	**H**	-	-	3.681	21.020
Ana	-	-		-	-	-	**Ka**	-	-	3.586	71.620
Br	3.514	10.170	3.514	21.180	3.523	4.490	**An**	3.524	9.080	-	-
Go	-	-	-	-	3.514	-	-	-	-	-	-
I	3.336	-	-	-	-	-	**I**	3.323	7.940	-	-
H	2.697	3.130	-	-	2.697	-	**H**	-	-	2.706	100.000
H	-	-	-	-	2.514	-	**H**	-	-	2.516	86.090

Gi	2.457	11.170	-	-	2.443	1.380	**Br**	2.459	11.810	-	-
Gi	-	-	-	-	-	-	**Gi**	-	-	-	-
Gi	2.455	-	2.452	28.890	2.418	3.960	**Gi**	2.386	6.870	-	-
Gi	2.375	7.320	2.383	14.330	2.386	2.870	**H**	-	-	2.206	34.220
Ka	-	-	-	-	-	-	**Gi**	2.048	5.790	-	-
H	-	-	-	-	-	-	**Br**	-	-	-	-
Gi	2.045	4.230	2.158	7.320	-	-	**Gi**	1.995	3.780	-	-
Gi	-	-	2.045	6.800	2.045	-	**Gi**	1.917	1.950	-	-
Gi	1.996	3.270	1.998	4.940	1.996	-	**H**	-	-	1.840	24.360
Gi	1.803	2.650	1.802	3.090	-	-	**Gi**	1.805	4.400	-	-
H	-	-	-	-	1.841	-	**Gi**	1.751	3.210	-	-
Q	-	-	-	-	-	-	**H**	-	-	-	-
H	-	-	-	-	-	-	**Gi**	1.687	6.550	-	-
Q	-	-	-	-	-	-	**H**	-	-	1.484	-
H	-	-	-	-	-	-	**Gi**	1.457	3.050	-	-
Gi	1.458	2.960	1.457	3.410	1.458	-	**H**	-	-	1.490	36.450
H	-	-	-	-	-	-	**H**	-	-	1.452	32.340

Gi= Gibbite, Go = Goethite, K=Kaolinite, Ana =Anatase, H=Hematite, Br= Brookite, Q=Quartz.

Table 3. Standard OH and Al-O-H stretching and bending frequencies compared with bauxite samples of present study

		Gamdapara Mines					**DN4W8-I**				**DN5W6-III**		
Minera Phase	**Gibbsite***	**LB-12**	**B-13**	**B-14**	**LB-15**	**G5**	**B-1**	**B-2**	**LB-3**	**L-4**	**B-5**	**LB-6**	**L-7**
v (OH)	3617, 3520,		3626	3624	3623	3624	3624	3624	3622	3622	3624	3622	3623
	3428, 3380												
δ(OH)	1024, 1060	1026				1017				1020		1013	1021
	958, 969	930								935			
	914												
y˙(OH)	802	810											
	743												
	Pure, Kaolinite**												
v(OH)	3695, 3889	3700			3695	3695			3694	3694		3695	3695
	3653, 3620,												
	3468												
H-O-H	1632-1645	1637	1642	1640	1637	1642	1645	1642	1641	1641	1632	1641	1641
bending of water													
Si-O vibration	1117-05	1114	1120	1122	1117	1114	1111	1117	1108	1111	1122	1109	1111
Si-O stretching	1019-5												
	940-35												
OH deformation linked to 2Al+3 Si-O quartz	918-09*** 700-686***	709	717		720			697	720	717	714	725	717
Si-O-Al strecthing	542-35***												
	Goethite												
	3095-2985												
	1660												
	1105												

	1040												
	912-882		896	907	893	938	895	893		935	981	938	944
	812-793												
	672												
	599-578												

*Gadsen, J. A. 1975., Kloprogge, J T, Raun, H D, and Frost, R L; 2002, **Silva, FANG, Medeiros, M I, Sampaio, J A, Santos, R D, Carnerio, M C, Costa, L S, and Garrido, M S, (2009). ***Saikia, B. J. and Parthasarathy, G.(2010)

Table 4. DTA peaks, TGA data of the samples of study area.

Sample No.	DTA Endothe-rmic Peaks	Thermogravimetry				Mineral Phase
		Initial wt. (mg)	Wt. loss (mg)	Temp (^{0}C)	Wt. loss (in %)	
B-1	325 ^{0}C	33.376	0.07 7.00 1.60	240 340 540	0.20 20.97 4.79	Gibbsite
B-2	320 ^{0}C	23.323	0.28 4.59 1.25	260 330 530	1.20 19.68 5.35	Gibbsite
B -5	300 ^{0}C	11.776	0.47 2.30 0.55	200 315 510	3.99 19.53 4.67	Gibbsite
LB-3	315 ^{0}C	24.658	0.36 4.15 1.36	275 335 530	1.45 16.83 5.51	Gibbsite
L-4	310 ^{0}C	16.951	0.25 2.10 0.70	265 320 520	1.47 12.38 4.12	Gibbsite

Table 5. B: Order of abundance of minerals

Sample No.	Sample Type	Order of abundance of Minerals based on peak intensity
B -1	Bauxite	Gibbsite >>> Brookite
B -2	Bauxite	Gibbsite >>> Brookite
B -5	Bauxite	Gibbsite >>> Ilmenite = Anatase
B -8	Bauxite	Gibbsite >>> Brookite= Anatase
B -9	Bauxite	Gibbsite >>> Anatase
B -13	Bauxite	Gibbsite >>> Brookite > Ilmenite
B -14	Bauxite	Gibbsite >>> Brookite
B -21	Bauxite	Gibbsite >>> Brookite >Anatase> Boehmite
B -23	Bauxite	Gibbsite >>> Brookite
LB -3	Lateritic Bauxite	Gibbsite >>> Brookite
LB – 6	Lateritic Bauxite	Hematite > Goethite > Gibbsite = Kaolinite

LB -10	Lateritic Bauxite	Gibbsite >> Hematite
LB -12	Lateritic Bauxite	Hematite > Ilmenite > Quartz
LB -15	Lateritic Bauxite	Gibbsite >> Brookite > Hematite
LB -20	Lateritic Bauxite	Gibbsite >>> Hematite > kaolinite > Boehmite
LB -22	Lateritic Bauxite	Gibbsite >> Hematite > Quartz > kaolinite
L -7	Laterite	Hematite > kaolinite > Goethite
L-4	Laterite	Hematite >>> kaolinite
G-5	Laterite	Hematite >>> Kaolinite

V. ACKNOWLEDGEMENT

We wish to express our sincere gratitude to the officers of Balco for providing logistics support during the field work. Assistance during fieldwork provided by the Mr. is also gratefully acknowledged. We are also thankful to Dr. B. K. Mohapatra for his valuable suggestions and to IMMT Bhubaneswar, NIT Raipur, for analysis work. We are also grateful to the Head SOS Geology and WRM for necessary laboratory facilities.

VI. REFERENCES

[1]. Deer,W.A.,Howie,R.A. and Zussmann,J. 1975. Rock-forming minerals,Orient Longmans,Vols. 1 to 5.

[2]. Gadsen,J. A. 1975. Infra-red spectra of minerals and related inorganic compounds,Butterworths,ISBN-0408-70665-1.

[3]. Gu,Jing.,Huang,Z.,Fan,H.,Jin,Z.,Yan, Z.,and Zhang,J. 2013. Mineralogy,geochemistry and genesis of lateritic bauxite deposits in the Wuchuan-Zheng'an-Daozhen area,Northen Guizhou Province,China. Jour. Geochemical Exploration. VOL. No. 130,44-59.

[4]. Jagannatha Rao J. and Krishnamurthy C. V. 1981. Some observations on the mineralogy and geochemistry of Hazaridadar and Raktidadar plateaus,Amarkantak Area,Madhya Pradesh,India. Proceeding of seminar on lateritization Processes,Oxford IBH Publication Co. New Delhi p. 89-103.

[5]. Kloprogge,J. T.,Raun,H. D. and Frost R.L. 2002. Thermal decomposition of bauxite minerals: Infrared emission spectroscopy of gibbsite,boehmite and diaspore. Jour. Material Sciences. VOL. No. 37,1121-1129.

[6]. Ruan,H.D.,Frost,R.L.,Kloprogge,J.T.,and Duong,L. 2002. Far-infrared spectroscopy of alumina phases. Spectrochimica Acta Part A 58, 479–491.

[7]. Saikia,B. J.,Parthasarathy,G.2010. Fourier Transform Infrared Spectroscopic Characterization of Kaolinite from Assam and Meghalaya,Northeastern India. J. Mod. Phys. VOL. No. 1,206-210. Doi:10.4236/jmp.2010.14031

[8]. Silva,F. A. N. G.,Medeiros,M. E.,Sampaio,J. A.,Santos,R. D.,Carnerio,M. C.,Costa,L. S. and Garrido,M. S. 2009. Technologocal characterization of Bauxite from Para-Brazil. CETEM,2009-018-00,San Francisco,14 a 19.

[9]. Valeton,I. D. A. 1972. Bauxites: Developments in soil sciences,Elsevier Pub. Co.,Amsterdam, 226 p.